

# **FLEXURAL ANALYSIS OF PRESTRESSED CONCRETE MONOBLOCK SLEEPERS FOR HEAVY-HAUL APPLICATIONS: METHODOLOGIES AND SENSITIVITY TO SUPPORT CONDITIONS**

**Henry E. Wolf**

Graduate Research Assistant  
University of Illinois, Urbana, IL, USA

**Marcus S. Dersch**

Senior Research Engineer  
University of Illinois, Urbana, IL, USA

**J. Riley Edwards**

Senior Lecturer and Research Scientist  
University of Illinois, Urbana, IL, USA

**Christopher P.L. Barkan**

Professor  
University of Illinois, Urbana, IL, USA

## **SUMMARY**

Throughout the international railway community, many methods have been developed to analyze the flexural demand of concrete sleepers. Specifically, this paper will focus on how changes in support condition assumptions affect the flexural analysis of the sleeper. The current flexural analysis methodologies contained in American Railway Engineering and Maintenance-of-Way Association (AREMA) Chapter 30, EuroNorm (EN) 13230, International Union of Railways (UIC) 713R, and Australian Standard (AS) 1085.14 will be explained and compared. To investigate the theoretical bending moments experienced by the sleeper under varying support conditions, a linear-elastic sleeper analysis model was developed. This model was used to perform a parametric study to determine the sensitivity of the sleeper to changes in ballast reaction along the sleeper. The results of this parametric study were compared to existing design recommendations to find allowable levels of ballast reaction that can occur beneath the sleeper before failure is expected. This model was also used to calculate theoretical bending moment values under ballast reactions measured in the field. Based on the results of these analyses, recommendations to improve current design and maintenance practices for prestressed concrete sleepers will be presented.

## INTRODUCTION

Throughout the world, the majority of railroad track infrastructure is supported by ballast. A ballasted track system typically consists of rail, fastening systems, sleepers, ballast, sub-ballast, and subgrade. The most commonly used material for sleepers in the United States is timber, which is used in about 90-95% of the sleepers in revenue service [1]. Concrete is the second most common material for sleepers, making up most of the remaining 5-10%. Steel and composite sleepers are also used, but they make up a negligible share of the number of sleepers in service. Typically, concrete sleepers are used in the most demanding service conditions (e.g. high curvature, steep grades, heavy tonnage, high speed passenger traffic, etc.)

As a material, concrete is very weak in tension, but very strong in compression. Because of this, concrete sleepers must be held in compression, or “prestressed”, with tensioned steel [2]. This can be achieved by tensioning steel wires or strands before or after the concrete is cast; members made this way are referred to as “pre-tensioned” and “post-tensioned”, respectively. Pre-tensioning is the more common practice for the manufacture of prestressed concrete sleepers in the United States. Prestressing significantly increases concrete’s flexural strength, ductility, and resistance to cracking. With this improved strength and ductility, prestressed concrete sleepers can withstand the demanding dynamic loading environment imparted by passing trains [2, 3].

The primary purpose of the sleeper is to maintain track geometry (e.g. gauge, cross level, etc.) and to transfer applied loads to the track substructure [4]. When a concrete sleeper supported on ballast is loaded vertically, the load is transferred from the wheel to the track system through the rail, fastening system, sleeper, ballast, sub-ballast, and subgrade. The ballast support conditions play a critical role in the type and severity of bending that the sleeper will experience under loading from a passing train [5]. The ballast support is affected by a variety of factors that include loading during train operations, tamping, fouling, and voids.

According to a survey of railroads, concrete sleeper manufacturers, and researchers from around the world, sleeper cracking from center binding was ranked as the third most critical problem with concrete sleepers [6]. North American respondents considered center cracking to be slightly less critical than their international counterparts, ranking it as the fifth most critical issue in concrete sleepers. However, North American respondents ranked cracking from dynamic loads as the third most critical issue, one place ahead of international respondents.

## NOTATION

$M_{RS+}$	rail seat positive bending moment
$M_{RS-}$	rail seat negative bending moment
$M_{C+}$	center positive bending moment
$M_{C-}$	center negative bending moment
$B$	unfactored rail seat positive moment (AREMA C30)
$V$	speed factor (AREMA C30, UIC 713R)
$T$	tonnage factor (AREMA C30)
$R$	design rail seat load
$WL$	unfactored wheel load
$DF$	distribution factor (AREMA C30, UIC 713R, AS 1085.14)
$IF$	impact factor (AREMA C30, AS 1085.14)
$w$	distributed ballast reaction
$L$	sleeper length
$g$	rail center spacing
$\gamma_p$	rail pad attenuation factor (UIC 713R)
$\gamma_r$	reaction support fault factor (UIC 713R)
$\gamma_i$	support irregularity factor (UIC 713R)
$f$	width of rail base
$h$	height of sleeper
$\alpha$	center reaction reduction coefficient
$b$	width of reduced center reaction

## CURRENT DESIGN METHODOLOGIES

The structural design process for prestressed concrete sleepers consists of two steps. First, an analysis is performed to estimate the demand (i.e. flexure, shear, etc.) that a structural element is expected to undergo in its lifetime. Second, the element is designed to meet or exceed the demand found in the analysis. Currently, design standards produced by organizations such as the American Railway Engineering and Maintenance-of-way Association (AREMA) [7], EuroNorm (EN) [8], International Union of Railways (UIC) [9], and Australian Standard (AS) [10] only provide formal recommendations on the analysis portion of the structural design process. In this section, an explanation and comparison of the analysis methodologies proposed by AREMA, EN, UIC, and AS will be provided. A clear understanding of these different methodologies and their respective assumptions is critical in improving the current structural design process for prestressed concrete monoblock sleepers.

### 1. AREMA C30

The current AREMA method for concrete sleeper flexural analysis is a factored approach that is dependent on sleeper length, sleeper spacing, annual tonnage, and train speed. Design bending moments are given for

four key locations on the sleeper: rail seat positive ( $M_{RS+}$ ), rail seat negative ( $M_{RS-}$ ), center positive ( $M_{C+}$ ), and center negative ( $M_{C-}$ ). To begin, AREMA Figure 30-4-3 is used to determine the factored design bending moment for a given loading condition. By specifying the sleeper spacing and the sleeper length, an unfactored rail seat positive bending moment ( $B$ ) can be found from AREMA Figure 30-4-3. AREMA Figure 30-4-4 is then used to determine the speed ( $V$ ) and tonnage factors ( $T$ ), which are based on expected track speed and tonnage, respectively. These three values are multiplied together using Equation 1. For each figure, linear interpolation can be performed between two specified points to obtain a more accurate factor.

$$M_{RS+} = B \times V \times T \quad (1)$$

Once the design rail seat positive bending moment is determined, it is multiplied by other factors to determine design bending moments at the three other key locations. The factors are based on sleeper length and can be linearly interpolated (AREMA Table 30-4-1).

The origins of AREMA Figure 30-4-3 are unclear, but a paper by McQueen [11] suggests that the chart is based on a 2.6 m (102 in) sleeper with 1524 mm (60 in) rail center-to-center spacing under a 365 kN (82 kip) axle load, as pictured in Figure 1a. The ballast reaction is assumed to be uniform along the entire length of the sleeper. The rail seat load is computed according to the AREMA recommendation, using Equation 2 below.

$$R = WL \times DF \times (1 + IF) \quad (2)$$

Thus, for a 365 kN (82 kip) axle load, 610 mm (24 in) sleeper spacing, and 200% impact factor, the design rail seat load is 276.2 kN (62.1 kip).

Because the ballast reaction is assumed to be uniform along the entire sleeper, the reaction can be found by multiplying the design rail seat load by two (to account for both rail seats) and then dividing by the length of the sleeper. So, for a 2.6 m (102 in) sleeper with a design rail seat load of 276.2 kN (62.1 kip), the distributed ballast reaction is 213 kN/m (1.22 k/in). McQueen then calculates the rail seat bending moment by modeling the end of the sleeper to the design rail seat load as a cantilever, using Equation 3 below.

$$M = \frac{w(L - g)^2}{8} \quad (3)$$

McQueen then applies a 10% factor to account for prestress losses. Most concrete sleeper manufacturers consider prestress losses in their design, meaning this increase of 10% is essentially a safety factor. After this

factor is applied, the product is rounded up to the nearest 0.6 kNm (5 k-in) to get the design rail seat positive bending moment. By applying this safety factor and rounding, the design rail seat positive bending moment proposed by McQueen is 33.9 kNm (300 k-in). This value matches the bending moment value given by AREMA Figure 30-4-3 for a 2.6 m (102 in) sleeper at 610 mm (24 in) spacing.

This design rail seat positive bending moment is then multiplied by factors in AREMA Table 30-4-1 to find values for design bending moments at the other critical regions. For a 2.6 m (102 in) sleeper, AREMA specifies a factor of 0.67 to calculate center negative bending moment. Thus, using the 33.9 kNm (300 k-in) rail seat positive bending moment, the center negative bending moment is 22.7 kNm (201 k-in). For a 2.6 m (102 in) sleeper with 1524 mm (60 in) rail center-to-center spacing, this center negative bending moment can be found when the reaction at a 448 mm (18 in) center section is reduced 39% (Figure 1b). These support conditions were found considering the 10% safety factor. It is also important to remember that these design bending moment values would then be multiplied by a tonnage and train speed factor, which could increase the values by as much as a factor of 1.32.

## 2. UIC 713R

EN 13230-1 states that the purchaser must specify the design bending moments to the sleeper manufacturer. In Annex E, it defers the analysis of design bending moments to UIC 713R. The UIC 713R method of analysis is dependent on sleeper length, sleeper spacing, axle load, rail pad attenuation, and train speed. Like AREMA, UIC also provides a pair of safety factors, one to account for "variation in sleeper reaction due to support faults" and another to account for "irregularity in the support along the sleeper." These factors are combined to result in a total impact factor of 3.24, the highest of the reviewed methodologies.

As seen previously in McQueen's method, the design rail seat load must first be calculated in order to perform the flexural analysis of the sleeper. The sleeper is assumed to be under a "newly tamped" condition, with the ballast reaction occurring symmetrically about the rail seat load (Figure 1c). Equation 4 below is used to calculate the design rail seat load according to UIC 713R.

$$R = WL \times DF \times [(1 + \gamma_p V) \gamma_r \gamma_i] \quad (4)$$

Thus, for a 365 kN (82 kip) unfactored axle load and the UIC 713R-recommended factors, the design rail seat load found according to

UIC 713R is 295.4 kN (66.4 kip), or 7% greater than the AREMA recommendation.

Next, UIC 713R calculates the rail seat positive bending moment for the sleeper with Equation 5.

$$M_{RS+} = \frac{R}{8}(L - g - f - h) \quad (5)$$

There are several assumptions made in this equation. First, the rail seat load is assumed to be uniformly distributed over the entire width of the rail base. As seen in research conducted at the University of Illinois at Urbana-Champaign (UIUC), this assumption is not necessarily valid, especially in the presence of lateral loads and high lateral to vertical (L/V) load ratios [12]. The distributed rail seat load causes the moment at the center of the rail seat to be reduced, which is explained in further detail by Freudenstein [13]. Additionally, UIC 713R assumes that the sleeper behaves as a deep beam, transferring the rail seat load in a compressive field spreading at a 45 degree angle to the neutral axis of the sleeper (assumed in the above equation to be one-half of the sleeper height). This means that for a 229 mm (9 in) deep sleeper supporting a rail base 152 mm (6 in) wide, the rail seat load is distributed over a length of 381 mm (15 in). This causes a significant reduction in moment. Thus, for a sleeper of length of 2.6 m (102 in), depth of 229 mm (9 in), and rail center-to-center spacing of 1524 mm (60 in), under an 365 kN (82 kip) unfactored axle load on a 152 mm (6 in) rail base the design rail seat positive bending moment per UIC 713R is 25.3 kNm (224 kip-in), a 25% reduction from the AREMA recommendation.

UIC 713R calculates the center negative bending moment using three methods. First, Equation 6 can be used for a sleeper with constant width. Two alternative equations can be used for sleepers with waisted (i.e. narrow) center sections, both of which account for a reduction in the center negative bending moment.

$$M_{C-} = \frac{R}{2} \left( g - \frac{2L^2 - b^2}{2(2L - b)} \right) \quad (6)$$

This equation takes a 50% reduction in center reaction into account with the term “b”, as seen in UIC 713R Figure 1, case b. UIC recommends this “partially consolidated” support condition for constant-width sleepers, but ultimately leaves the center reaction reduction to the discretion of the sleeper purchaser. Freudenstein [13] uses the assumption that there is no reduction in the center reaction and that there is a uniform ballast reaction along the entire length of the

sleeper (b=0 mm) as shown in Figure 1d. The center negative bending moment can be found by modelling the sleeper as a cantilevered beam fixed at the sleeper center with a rail seat load acting downwards and the ballast reaction acting upwards. Thus, for a constant-width sleeper of length 2.6 m (102 in) and 1524 mm (60 in) rail center-to-center spacing, under an 365 kN (82 kip) unfactored axle load, the design center negative bending moment per UIC 713R is 33.8 kNm (299 kip-in), a nearly 50% increase from the AREMA recommendation. After the design rail seat positive and center negative bending moments are calculated, they are multiplied by factors of 0.5 and 0.7, respectively, to get design rail seat negative and center positive bending moments.

### 3. AS 1085.14

The current AS method for sleeper flexural analysis is dependent on sleeper length, sleeper spacing, and axle load. As in the previously demonstrated methods, the rail seat load must first be computed. AS 1085.14 proposes an equation that is very similar to the AREMA recommendation, seen in Equation 7.

$$R = IF \times WL \times DF \quad (7)$$

Thus, assuming the minimum impact factor of 2.5, under a 365 kN (82 kip) axle load and 610 mm (24 in) sleeper spacing, the design rail seat load is 237.2 kN (53.3 kip). One difference between this method and AREMA are the magnitudes of the impact and distribution factors. AREMA calls for a 200% impact factor, but this factor is added to 1.0 such that the true impact factor is 3.0, compared to the 2.5 used in AS 1085.14. If AS expressed this impact factor in the same manner as AREMA, it would be 150%. An impact factor of 150% was used by AREMA in the past, but it was since raised to its current value of 200% [14]. Another difference is seen in the distribution factor figures (AREMA Figure 30-4-1 and AS1085.14 Figure 4.1), which give slightly different values, approximately 50.5% and 52% for AREMA and AS, respectively. AS 1085.14 and AREMA C30 both differ from UIC 713R by not including reductions for rail pad attenuation or safety factors to account for support irregularities or voids. UIC 713R also does not consider load distribution from rail to rail seat as rigorously, using a factor of 0.5 if the rail section is heavier than 46 kg/m (93 lbs/yd) and the sleeper spacing is less than 650 mm (25.6 in).

To calculate the design rail seat positive bending moment, AS 1085.14 uses the same support conditions as UIC 713R, assuming the

“newly tamped” condition shown in Figure 1e. However, AS 1085.14 treats the rail seat load as a point load and neglects deep beam behavior, which is similar to McQueen’s analysis. This assumption also slightly simplifies the calculation, as seen in Equation 8.

$$M_{RS+} = \frac{R(L - g)}{8} \quad (8)$$

Thus, for a sleeper of length of 2.6 m (102 in) and rail center-to-center spacing of 1524 mm (60 in), under a 365 kN (82 kip) unfactored axle load, the design rail seat positive bending moment per AS 1085.14 is 31.6 kNm (280 kip-in), a 7% reduction from the AREMA recommendation and a 25% increase from the UIC recommendation.

The AS 1085.14 center negative analysis is very similar to the UIC 713R analysis presented earlier. Both assume uniform ballast reaction along the length of the sleeper, but AS treats the rail seat load as a point load (Figure 1f). As a result, the AS 1085.14 equation for design center negative bending moment (Equation 9), is the same as the UIC 713R equation for design center negative bending moment (Equation 6) when there is no center reaction reduction ( $b=0$  mm).

$$M_{C-} = \frac{R(2g - L)}{4} \quad (9)$$

Thus, for a sleeper of length 2.6 m (102 in) and 1524 mm (60 in) rail center-to-center spacing, under a 365 kN (82 kip) unfactored axle load the design center negative bending moment per AS 1085.14 is 27.1 kNm (240 kip-in), a 20% increase from the AREMA recommendation and a 20% reduction from the UIC recommendation.

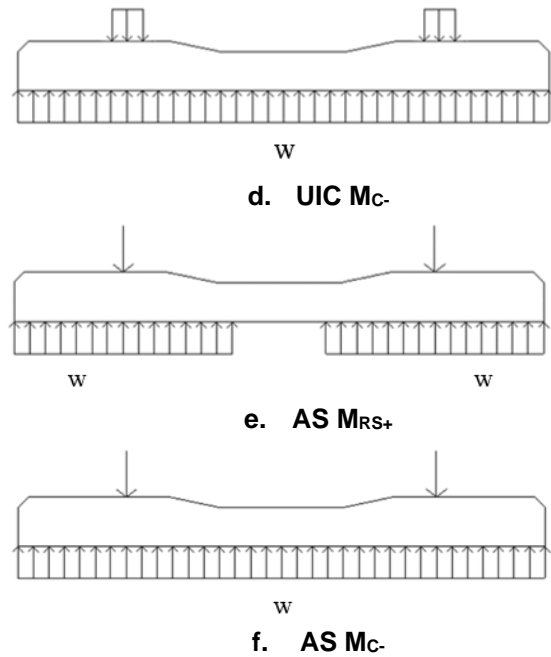
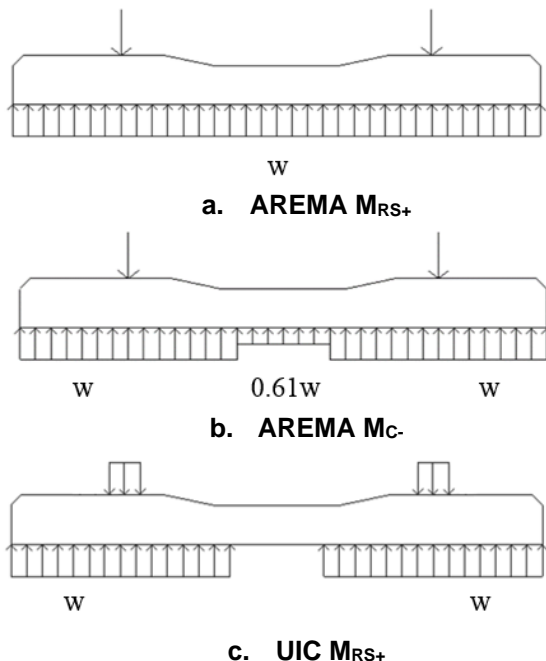


**Figure 1: Support Conditions for Selected Design Recommendations**

Table 1 provides a comparison of the results found using the different analysis methods explained above. The maximum bending moment found from the analyses for each critical region is highlighted. A model to quickly and easily perform flexural analysis for a sleeper under varying support conditions is needed to further distinguish between these methodologies, and is developed and presented in the next section.

**Table 1: Comparison of Flexural Analysis Methodologies**

		AREMA	UIC	AS
WL	kN (kip)	365 (82)	365 (82)	365 (82)
L	m (in)	2.6 (102)	2.6 (102)	2.6 (102)
g	mm (in)	1524 (60)	1524 (60)	1524 (60)
f	mm (in)	152 (6)	152 (6)	152 (6)
h	mm (in)	229 (9)	229 (9)	229 (9)
Sleeper Spacing	mm (in)	610 (24)	610 (24)	610 (24)
DF		50.5%	50%	52%
IF		3.00	3.24	2.50
R	kN (kip)	277.2 (62.1)	295.4 (66.4)	237.2 (53.3)

$M_{RS+}$	kNm (k-in)	33.9 (300)	25.3 (224)	31.6 (280)
$M_{RS-}$	kNm (k-in)	18.0 (159)	12.7 (112)	21.1 (187)
$M_{C+}$	kNm (k-in)	15.9 (141)	23.6 (209)	12.7 (112)
$M_{C-}$	kNm (k-in)	22.7 (201)	33.8 (299)	27.1 (240)

**SLEEPER ANALYSIS MODEL**

In order to better understand the effect of changing support conditions on sleeper bending moments, it was necessary to develop an analytical model. The authors desired to create a model that was easily accessible and simple to use. As such, Microsoft Excel was chosen as the platform for this tool and basic Euler-Bernoulli beam theory was used.

To further simplify the analysis, half of the sleeper was modeled as a linear-elastic cantilevered beam. This assumed that the sleeper was symmetrically loaded and supported about the center, and that the loading was quasi-static. The ballast reaction was modeled as a distributed load and the rail seat load was modeled as a point load (as seen in the AREMA and AS analyses). This model was developed for a sleeper with a length of 2.6 m (102 in) and rail center-to-center spacing of 1524 mm (60 in), but can accommodate varying sleeper lengths and rail center-to-center spacings.

In order to quickly adjust the ballast reaction, the reaction was split into sections or “bins”. These bins were placed symmetrically about the rail seat load in order to easily simulate different theoretical and experimental ballast reactions. Dividing the rail seat supported section into six bins was deemed to provide adequate resolution. For a 2.6 m (102 in) sleeper, this meant that each rail seat bin was 177.8 mm (7 in). This left a 228.6 mm (9 in) section at the sleeper center, which was split into three bins for consistency and to provide greater resolution at the region expected to be most critical to the center bending moment. Figure 2 shows the set-up of this sleeper model with the ballast reaction split into nine bins.

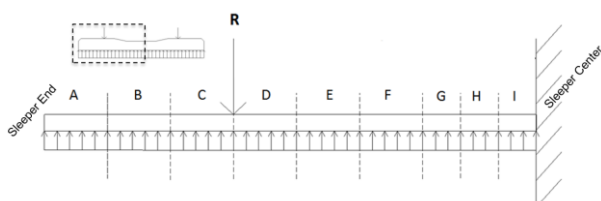


**Figure 2: Illustration of Sleeper Bending Model**

**EFFECT OF SUPPORT CONDITIONS ON SLEEPER BENDING MOMENTS**

The goal of the parametric study was to determine the bending moment values that could be experienced by a sleeper under a given rail seat load and different support conditions. First, this problem was bounded by idealizing the ballast reaction as a point load that varies with “x” along the length of the sleeper, as given in Equation 10. This idealization assumes that the entire rail seat load is taken by a single discrete point underneath the sleeper. It would be similar to a sleeper being supported symmetrically about the center by two pieces of ballast.

$$M_C = -R \left( \frac{g}{2} \right) + P_x \tag{10}$$

For a rail seat load of 276.2 kN (62.1 kip) on a sleeper with length of 2.6 m (102 in) and a rail center-to-center spacing of 1524 mm (60 in), the theoretical bending moment extremes at the sleeper center could range from 147.3 kNm (1304 kip-in) to -210.5 kNm (-1863 kip-in), where the maximum positive moment occurs when the reaction load occurs at the end of the sleeper and the maximum negative moment occurs when the reaction load occurs at the center of the sleeper. These values are the upper and lower limits of bending moments that could be experienced by the sleeper. However, this method is overly simplified and does not provide realistic support conditions.

**Table 2: Effect of Ballast Reaction on  $M_{RS}$  and  $M_C$**

Section	A	B	C	D	E	F	G	H	I	
Rail Seat Moment ( $M_{RS}$ ) kNm (k-in)	0%	15.6 (138)	23.4 (207)	31.3 (277)	35.1 (311)	35.1 (311)	35.1 (311)	32.2 (285)	32.2 (285)	32.2 (285)
	25%	42.4 (375)	36 (319)	29.6 (262)	26.3 (233)	26.3 (233)	26.3 (233)	24.2 (214)	24.2 (214)	24.2 (214)
	50%	69.3 (613)	48.6 (430)	27.9 (247)	17.6 (156)	17.6 (156)	17.6 (156)	16.2 (143)	16.2 (143)	16.2 (143)
	75%	96 (850)	61.1 (541)	26.2 (232)	8.8 (78)	8.8 (78)	8.8 (78)	8 (71)	8 (71)	8 (71)
	100%	122.8 (1087)	73.7 (652)	24.5 (217)	0 (0)	0 (0)	0 (0)	0 (0)	0 (0)	0 (0)
Center Moment ( $M_C$ ) kNm (k-in)	0%	-56.2 (-497)	-48.4 (-428)	-40.4 (-358)	-32.7 (-289)	-24.9 (-220)	-17.1 (-151)	-23.7 (-210)	-22.4 (-198)	-21.1 (-187)
	25%	-11.4 (-101)	-17.9 (-158)	-24.3 (-215)	-30.7 (-272)	-37.1 (-328)	-43.5 (-385)	-57.2 (-506)	-61.5 (-544)	-65.8 (-582)
	50%	33.3 (295)	12.8 (113)	-7.9 (-70)	-28.6 (-253)	-49.3 (-436)	-69.8 (-618)	-90.8 (-804)	-100.7 (-891)	-110.5 (-978)
	75%	78.1 (691)	43.2 (382)	8.4 (74)	-26.6 (-235)	-61.5 (-544)	-96.4 (-853)	-124.3 (-1100)	-139.8 (-1237)	-155.2 (-1374)
	100%	122.8 (1087)	73.7 (652)	24.5 (217)	-24.5 (-217)	-73.7 (-652)	-122.8 (-1087)	-157.8 (-1397)	-179 (-1584)	-200 (-1770)

To more realistically express the ballast reactions seen in track, the percentage of total reaction taken by each bin was modified. To compare the sensitivity of the reaction of each bin on the bending moments, each bin was modified separately, such that the ballast reaction in one bin changed and the ballast reactions in the other eight bins shared the remainder of the reaction equally. For example, if bin A takes 0% of the rail seat load, 100% of the ballast reaction would be shared equally between bins B-I. The rail seat and

center bending moments under these conditions are found to be 15.6 kNm (138 kip-in) and -56.2 kNm (-497 kip-in), respectively. Similarly, if bin C takes 25% of the rail seat load, the remaining 75% is split equally to bins A, B, and D-I, for a rail seat moment of 29.6 kNm (262 kip-in) and a center moment of -24.3 kNm (-215 kip-in). The complete results of this study are shown in Table 2. The rail seat load used in these analyses was 276.2 kN (62.1 kip).

From the above table, one can see how the shift in the ballast reaction affects the rail seat and center bending moments. As larger percentages of the ballast reaction are taken by bins closer to the sleeper end (A, B), the rail seat and center bending moments both increase, and vice versa. Shaded cells represent moments that exceed the maximum values found using any of the analysis methods explained previously (Table 1). It is seen that the rail seat bending moment is always positive and is very sensitive to changes in bins A, B, and C (i.e. the distance between the rail seat and the end of the sleeper). This is seen in the very high bending moments when the ballast reaction is concentrated at these bins. As discussed earlier, the magnitude of the center bending moment can be very high for either positive or negative bending. The center experiences its maximum positive bending moments when the ballast reaction is concentrated outside of the rail center-to-center spacing and experiences its maximum negative bending moments when the ballast reaction is concentrated inside of the rail center-to-center spacing.

One of the simplest ways to see the sensitivity of a bin is to compare the difference between moments found when the bin takes 0% and 100% of the ballast reaction. For the rail seat bending moment, the most sensitive bin is found to be bin A, where the difference between the moment when 100% of the ballast reaction occurs in bin A (122.8 kNm (1087 kip-in)) and when 0% of the ballast reaction occurs in bin A (15.6 kNm (138 kip-in)) is 107.2 kNm (949 kip-in). Since bin A is the free end located the greatest distance from the rail seat load, it has the largest moment arm and the greatest effect on bending at the rail seat. The least sensitive bin for rail seat bending moment is bin C, with a difference in the 0 and 100% reactions of only -6.8 kNm (-60 kip-in). This is because it has a smaller moment arm from the rail seat.

Continuing this method of comparison to the center bending moment, bin I has the greatest sensitivity, with a difference in the 0 and 100% reactions of -178.9 kNm (-1583 kip-in). As the reaction moves closer to the sleeper center, the distance between the rail seat load and the centroid of the reaction increases, causing greater magnitudes of negative bending. The center bending moment was found to be least affected by

changes in bin D, with a difference in the 0 and 100% reactions of only 8.2 kNm (72.6 kip-in).

When tracking the fairly realistic case of a bin taking 25% of the ballast reaction across the sleeper (from bin A to bin I, down the 25% rows in Table 2), it is clear how quickly center negative bending moments can exceed current design recommendations. As stated by Remennikov et al. [15] and frequently noted by North American concrete sleeper designers, most concrete sleepers are overdesigned and have reserve strength. Even so, if a sleeper was designed to meet UIC 713R, the most demanding center negative recommendation, this strength would be exceeded when bins E, F, G, H, or I take 25% or more of the ballast reaction. This shows how even small levels of center binding can potentially lead to center negative cracking.

Figure 3 further illustrates the change in bending moment at the sleeper center as the percent of ballast reaction in each bin changes. The maximum design bending moments found using current recommendations are also plotted to show the range in which cracking is not expected. It is easy to see the sensitivity of each bin by the slope of its line; higher slopes indicate greater sensitivity while lower slopes indicate less sensitivity. The intersection of the lines occurs when all of the bins take the same percent of the ballast reaction. Because of the difference in bin size, this occurs when bins A-F take 13.7% and bins G-I take 5.9%.

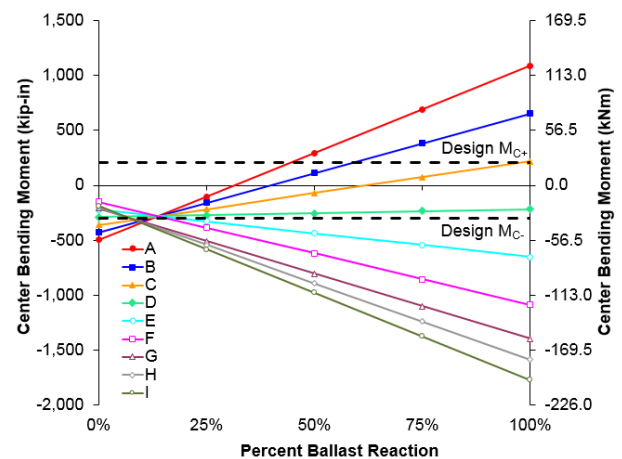
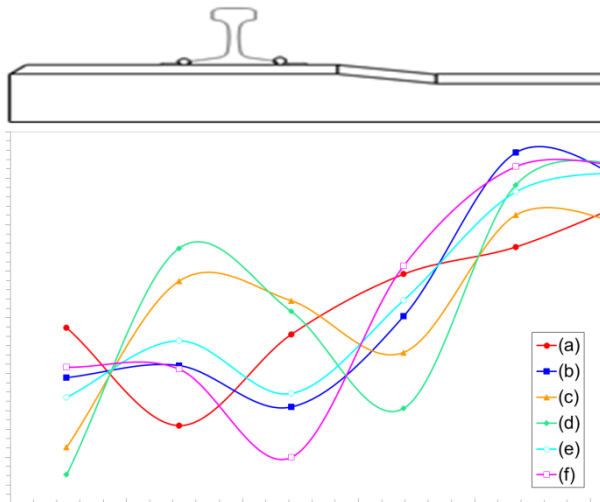


Figure 3: Center Bending Moment Under Changes in Ballast-Reaction

### SLEEPER BENDING MOMENTS FROM FIELD-MEASURED BALLAST REACTIONS

To better predict the magnitude of bending moments that could be seen in the field, support conditions found at Transportation Technology Center. (TTC) [16] were used in the sleeper analysis model. These support conditions are shown in Figure 4. None of the zones were tamped after application of ballast, but all zones underwent 1.5 MGT of traffic after installation.



**Figure 4: Support Conditions Experimentally Measured in the Field [16]**

To keep the analysis consistent, the measured ballast reactions were scaled to the rail seat load used in the parametric study of 276.2 kN (62.1 kip). These ballast reactions were then used in the sleeper analysis model to compute the bending moments at the rail seat and center. The results of these analyses are listed in Table 3.

**Table 3: Theoretical Bending Moments for Field-Measured Support Conditions**

Sleeper	$M_{RS}$	$M_C$
Fig. 4 (a)	41.1 kNm (364 kip-in)	11.9 kNm (105 kip-in)
Fig. 4 (b)	34.8 kNm (308 kip-in)	-8.6 kNm (-76 kip-in)
Fig. 4 (c)	44.6 kNm (395 kip-in)	2.4 kNm (21 kip-in)
Fig. 4 (d)	45.5 kNm (403 kip-in)	6.7 kNm (59 kip-in)
Fig. 4 (e)	41.0 kNm (363 kip-in)	6.9 kNm (61 kip-in)
Fig. 4 (f)	39.1 kNm (346 kip-in)	11.1 kNm (98 kip-in)

As seen in the table above, the theoretical rail seat bending moments found using these field-measured support conditions exceeded values from all design recommendations. In spite of this, none of the sleepers were found to have experienced flexural cracking. This is most likely due to the rail seat load experienced by the sleepers in this testing not reaching the 276.2 kN (62.1 kip) used in the analysis. This could also suggest that the sleepers were designed to be significantly stronger than suggested by current design recommendations. Another possibility is that the sleeper behaved as a deep beam and transferred the rail seat load to the ballast through a compressive field (as assumed in the UIC 713R

analysis), reducing the bending moment experienced at the rail seat.

The center bending moments found under these support conditions were all within design recommendations. This suggests that center cracking is not a concern under these support conditions and loading environment. It is important to remember that the support conditions measured in this study at TTC represent only a very small sample of conditions that could be found on a heavy-haul freight line in the United States.

### PROPOSED METHOD FOR SLEEPER FLEXURAL ANALYSIS

To calculate maximum bending moments, Equations 11 and 12 are proposed by the authors. These equations are calculated with a variable center support coefficient ( $\alpha$ ) and a uniformly distributed rail seat load. These equations are currently being reviewed by a committee of railroads, manufacturers, and academics to determine acceptable levels of center support, and will be proposed for inclusion in the 2015 AREMA recommended practices.

$$M_{RS} = \frac{1}{8} \left[ \left( \frac{2R}{2(L-g) + \alpha(2g-L)} \right) (L-g)^2 - Rg \right] \quad (11)$$

$$M_C = \frac{1}{2} R \left[ \frac{L^2 - (1-\alpha)b^2}{2(L - (1-\alpha)b)} - g \right] \quad (12)$$

### FIELD EXPERIMENTATION FOR SLEEPER BENDING MOMENTS

From past experiences, bending moments of concrete sleepers can be measured in the field with surface strain gauges. This is proposed to improve the understanding of sleeper flexural behavior and ballast support reactions.

To improve tamping cycles, it is desired to measure bending moments as tonnage accumulates on a rail line. These bending moment values can then be related to tonnage, noting the traffic required to cause center negative bending moments exceeding design recommendations. Figure 5 shows a hypothetical chart depicting the increase of center negative bending moments as tonnage accumulates on a rail line and the sleeper becomes increasingly center bound.

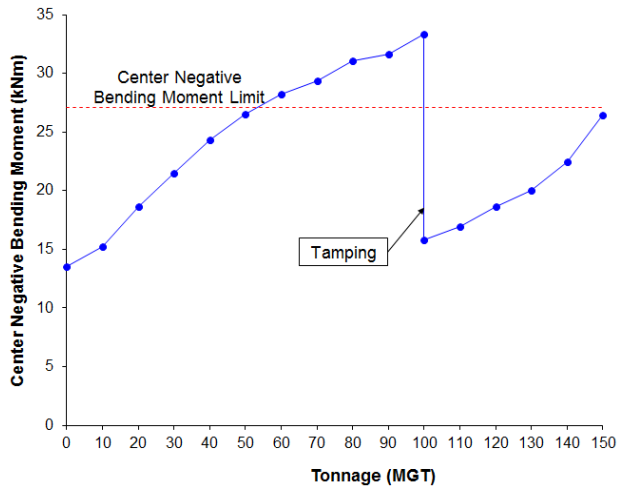


**Figure 5: Hypothetical Center Negative Bending Moments with Increased Tonnage**

To better understand the flexural behavior of the sleeper, five strain gauges can be used on each instrumented sleeper, as shown in Figure 6. These measured bending moments can help capture most of the sleeper bending behavior, including asymmetric wheel loading, lateral loads, and non-uniform ballast support conditions.

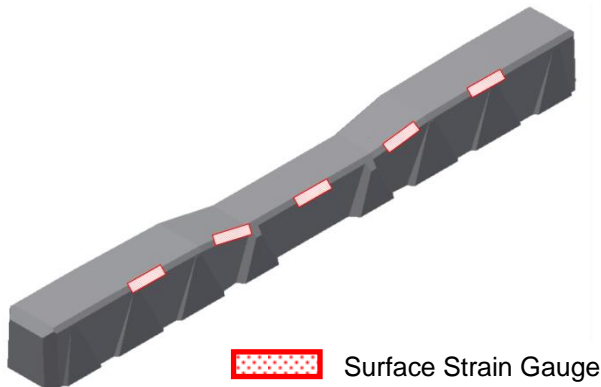


**Figure 6: Preliminary Instrumentation Plan**

These measured bending moments can also be used to estimate the reaction forces acting on the bottom of the sleeper. A MATLAB program is being developed that can provide back-calculated estimates of the sleeper support conditions using the sleeper length, rail center spacing, rail seat loads, and measured bending moments. This program estimates support by using a pattern search optimization algorithm to determine the support reactions that best match the measured bending moments. A sample of the final output of a known support condition is shown in Figure 7. This would provide a good estimate for support conditions experienced in the field and could be used to improve current flexural analysis methodologies and assumptions.

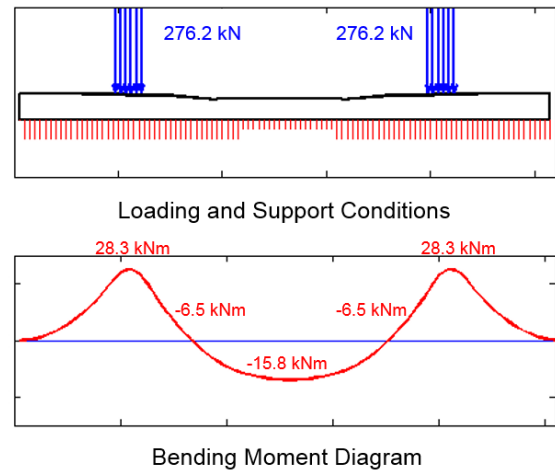


**Figure 7: Example Support Condition Back-Calculation Estimate for Concrete Sleeper**

## CONCLUSIONS

The flexural behavior of a concrete sleeper is highly dependent on the sleeper support conditions. Current design recommendations make different assumptions for these sleeper support conditions, which leads to different recommended design bending moments. The parametric study presented shows the high level of sensitivity of the center bending moment as a function of changing support conditions. Design bending moments at the sleeper center can be exceeded under small shifts in distribution of the ballast reaction. This demonstrates that frequent tamping to keep the ballast reaction concentrated under the rail seats can prevent very high center negative bending moments that cause cracking. This high sensitivity also suggests that current design recommendations for center bending moment may need to be increased. Sleeper span-to-depth ratios indicate that for rail seat positive bending the sleeper behaves as a deep beam, transferring load through a compressive field. As such, reductions in design bending moments for positive bending at the rail seat for both the AREMA and AS recommendations may be warranted. At the very least, treating the rail seat load as a point load is overly conservative. The assumption that the rail seat load acts over the entire width of the rail base is used in the proposed equations. For center negative bending the span-to-depth ratio is greater and the sleeper experiences closer to true flexure. The support condition assumptions used in current design recommendations did not correspond closely with the support conditions measured in field testing, which suggests that current support condition assumptions may need to be modified to more closely match field conditions.

## ACKNOWLEDGEMENTS

The authors would like to thank the National University Rail (NURail) Center, a US DOT-OST Tier 1 University Transportation Center and the Federal Railroad Administration (FRA) for providing funding for this project. The lead author has been supported in part by Amsted RPS. The published material in this paper represents the position of the authors and not necessarily that of DOT. The authors would like to extend their appreciation to the Transportation Technology Center, Inc. (Mike McHenry), voestalpine Nortrak (Steve Mattson), CXT Concrete Ties (Vince Peterson), GIC Ingeniería y Construcción (Mauricio Gutierrez and Ryan Kernes), KSA Concrete Ties (Ryan Rolfe), Rail.One GmbH (Arnold Pieringer and Wojciech Narwat), and Rocla Concrete Tie (Rusty Croley and Pedro Lemmert) for their helpful advice. The authors are also grateful for the advice and assistance provided by students and staff from RailTEC, especially Zhengboyang Gao. J. Riley Edwards has been supported in part by grants to the UIUC Railroad Engineering Program from CN, Hanson Professional Services, and the George Krambles Transportation Scholarship Fund. Industry partnership and support has been provided by Union Pacific Railroad; BNSF Railway; National Railway Passenger Corporation (Amtrak); Amsted RPS / Amsted Rail, Inc.; GIC; Hanson Professional Services, Inc.; CXT Concrete Ties, Inc., an LB Foster Company; and TTX Company.

## REFERENCES

- (1) M/W budgets to climb in 2008. *Railway Track & Structures* 2008;104(1): 18-25.
- (2) Zeman, J.C. Hydraulic mechanisms of concrete-tie rail seat deterioration. M.S. Thesis. University of Illinois at Urbana-Champaign; 2010.
- (3) Jimenez R, LoPresti J. Performance of alternative tie material under heavy-axle-load traffic. *Railway Track & Structures* 2004;100(1): 16-18.
- (4) Hay, WW. *Railroad engineering*. 2<sup>nd</sup> ed. New York: John Wiley and Sons; 1983.
- (5) Kaewunruen S, Remennikov AM. Investigation of free vibrations of voided concrete sleepers in railway track system. *Proceedings of the Institution of Mechanical Engineers, Part F: Journal of Rail and Rapid Transit* 2007;221(4): 495-507.
- (6) Van Dyk, B. J. Characterization of loading environment for shared-use railway superstructure in North America. M.S. Thesis. University of Illinois at Urbana-Champaign; 2013.
- (7) American Railway Engineering and Maintenance-of-Way Association. *Manual for railway engineering*. Lanham, Maryland: AREMA; 2014.
- (8) European Committee for Standardization. EN 13230-1. *Railway applications – track – concrete sleepers and bearers – Part 1: general requirements*. Brussels: EN; 2009.
- (9) International Union of Railways. UIC 713R. *Design of monoblock concrete sleepers*; 2004.
- (10) Standards Australia International. AS 1085.14. *Railway track material, part 14: prestressed concrete sleepers*; 2003.
- (11) McQueen PJ. *Introduction of concrete tie systems*. San Rafael, California; 1983.
- (12) Greve M, Dersch MS, Edwards JR, Barkan CPL, Mediavilla J, Wilson B. Analysis of the relationship between rail seat load distribution and rail seat deterioration in concrete sleepers. In: *ASME Joint Rail Conference 2-4 April 2014, Colorado Springs*.
- (13) Freudenstein S. Concrete ties designed for high dynamic loads. In: *Proceedings of the AREMA 2007 Annual Conference 9 – 12 September 2007, Chicago*.
- (14) McQueen PJ. *Flexural performance requirements for prestressed concrete ties by factoring*. San Rafael, California, 2010.
- (15) Remennikov AM, Murray MH, Kaewunruen S. Conversion of AS1085.14 for prestressed concrete sleepers to limit states design format. In: *AusRAIL PLUS 2007 Conference & Exhibition, 2 -8 December, Sydney*.
- (16) McHenry MT. Pressure measurement at the ballast-tie interface of railroad track using matrix based tactile surface sensors. M.S. Thesis. University of Kentucky; 2013.